

Molecular Cell, Volume 52
Supplemental Information

**PrimPol, an Archaic Primase/Polymerase
Operating in Human Cells**

**Sara García-Gómez, Aurelio Reyes, María I. Martínez-Jiménez, E. Sandra Chocrón,
Silvana Mourón, Gloria Terrados, Christopher Powell, Eduardo Salido, Juan Méndez, Ian
J. Holt, and Luis Blanco**

Species	Sequence	Species	Sequence	Species	Sequence		
Homo	...NDR--IQGIVLGGSSARL--IHLGEEFGKATYVLA...PITLTKSVFLNHSRSDVWIDVYSPFSLQREVENTYQYQKIVYR...LTELHGHV	Macaca	...NDR--IQGIVLGGSSARL--IHLGEEFGKATYVLA...PITLTKSVFLNHSRSDVWIDVYSPFSLQREVENTYQYQKIVYR...LTELHGHV	Bos	...NDR--IQGIVLGGSSARL--IHLGEEFGKATYVLA...PITLTKSVFLNHSRSDVWIDVYSPFSLQREVENTYQYQKIVYR...LTELHGHV	Equus	...NDR--IQGIVLGGSSARL--IHLGEEFGKATYVLA...PITLTKSVFLNHSRSDVWIDVYSPFSLQREVENTYQYQKIVYR...LTELHGHV

Species	Sequence	Species	Sequence	Species	Sequence		
Homo	...LSSVYVPL--SPEEPLSALFIRORNFVYKSCDHPVYLK--VGD--QITLITVYVYFYKSK--MLHC--YVLPENIKKYL...YVLRNPN--GRGAKGHVLLI...	Macaca	...LSSVYVPL--SPEEPLSALFIRORNFVYKSCDHPVYLK--VGD--QITLITVYVYFYKSK--MLHC--YVLPENIKKYL...YVLRNPN--GRGAKGHVLLI...	Bos	...LSSVYVPL--SPEEPLSALFIRORNFVYKSCDHPVYLK--VGD--QITLITVYVYFYKSK--MLHC--YVLPENIKKYL...YVLRNPN--GRGAKGHVLLI...	Equus	...LSSVYVPL--SPEEPLSALFIRORNFVYKSCDHPVYLK--VGD--QITLITVYVYFYKSK--MLHC--YVLPENIKKYL...YVLRNPN--GRGAKGHVLLI...

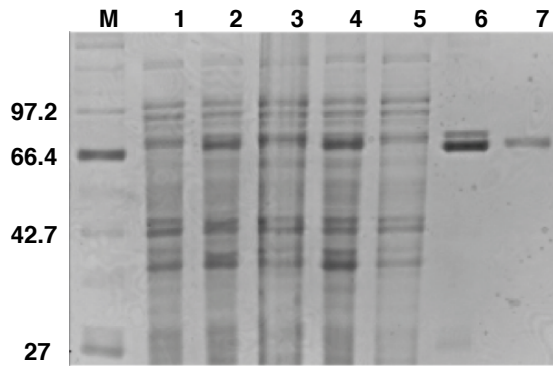
Species	Sequence	Species	Sequence	Species	Sequence		
Homo	...GFQNFHTEKTEEISAKSLERLGSREDSQSPSLFVYVWGGKIK...FVLLVYTRNRRLRYSKSLDTPYRRL--EYTD--NRFPTFDS--KVDS--DEYDFL...	Macaca	...GFQNFHTEKTEEISAKSLERLGSREDSQSPSLFVYVWGGKIK...FVLLVYTRNRRLRYSKSLDTPYRRL--EYTD--NRFPTFDS--KVDS--DEYDFL...	Bos	...GFQNFHTEKTEEISAKSLERLGSREDSQSPSLFVYVWGGKIK...FVLLVYTRNRRLRYSKSLDTPYRRL--EYTD--NRFPTFDS--KVDS--DEYDFL...	Equus	...GFQNFHTEKTEEISAKSLERLGSREDSQSPSLFVYVWGGKIK...FVLLVYTRNRRLRYSKSLDTPYRRL--EYTD--NRFPTFDS--KVDS--DEYDFL...

Species	Sequence	Species	Sequence	Species	Sequence		
Homo	...ELLVYDXY--KQENLGRKQK...-TILLVLYKNEYAKGQPKQPKNF--CSDCFLPHEVLLFLKEEEL--FTTIDG--EIKSMENAPKPPSPS...	Macaca	...ELLVYDXY--KQENLGRKQK...-TILLVLYKNEYAKGQPKQPKNF--CSDCFLPHEVLLFLKEEEL--FTTIDG--EIKSMENAPKPPSPS...	Bos	...ELLVYDXY--KQENLGRKQK...-TILLVLYKNEYAKGQPKQPKNF--CSDCFLPHEVLLFLKEEEL--FTTIDG--EIKSMENAPKPPSPS...	Equus	...ELLVYDXY--KQENLGRKQK...-TILLVLYKNEYAKGQPKQPKNF--CSDCFLPHEVLLFLKEEEL--FTTIDG--EIKSMENAPKPPSPS...

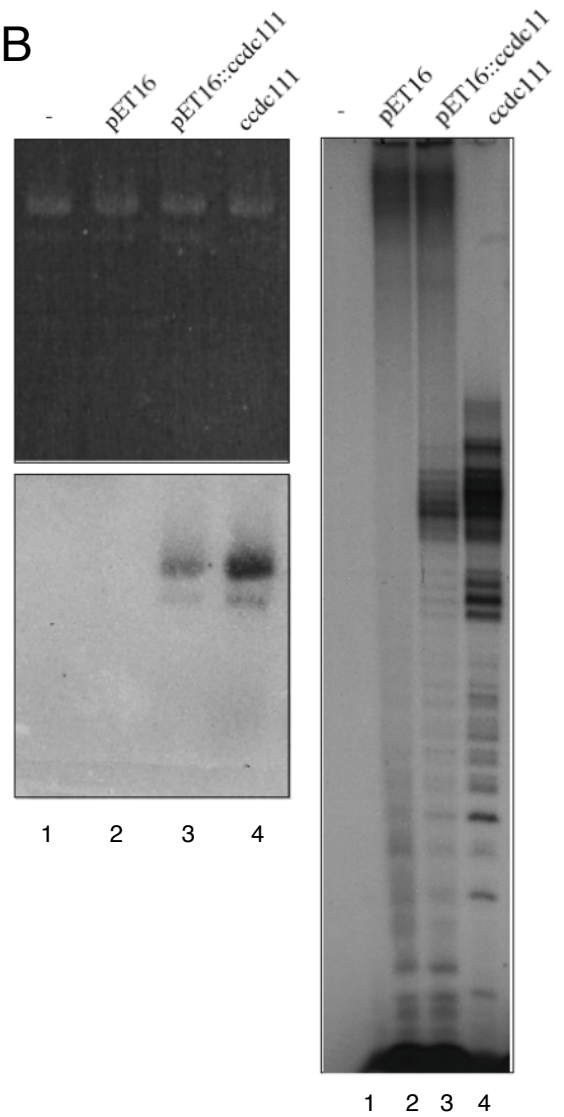
Species	Sequence	Species	Sequence	Species	Sequence		
Homo	...ELLVYDXY--KQENLGRKQK...-TILLVLYKNEYAKGQPKQPKNF--CSDCFLPHEVLLFLKEEEL--FTTIDG--EIKSMENAPKPPSPS...	Macaca	...ELLVYDXY--KQENLGRKQK...-TILLVLYKNEYAKGQPKQPKNF--CSDCFLPHEVLLFLKEEEL--FTTIDG--EIKSMENAPKPPSPS...	Bos	...ELLVYDXY--KQENLGRKQK...-TILLVLYKNEYAKGQPKQPKNF--CSDCFLPHEVLLFLKEEEL--FTTIDG--EIKSMENAPKPPSPS...	Equus	...ELLVYDXY--KQENLGRKQK...-TILLVLYKNEYAKGQPKQPKNF--CSDCFLPHEVLLFLKEEEL--FTTIDG--EIKSMENAPKPPSPS...

Fig S1 Garcia-Gomez et al.

A

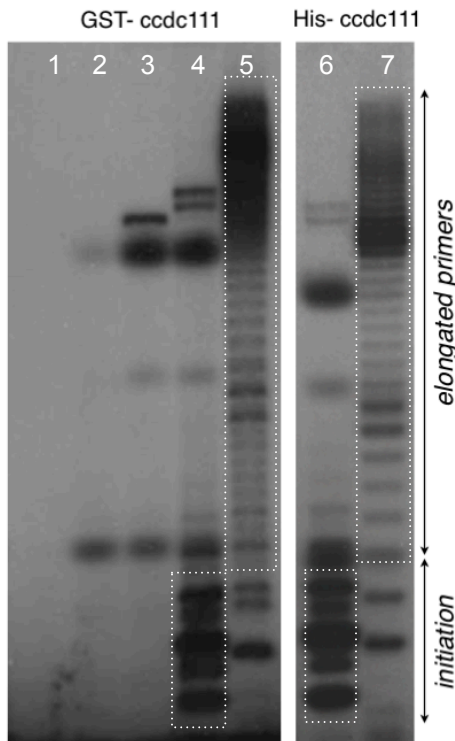


B



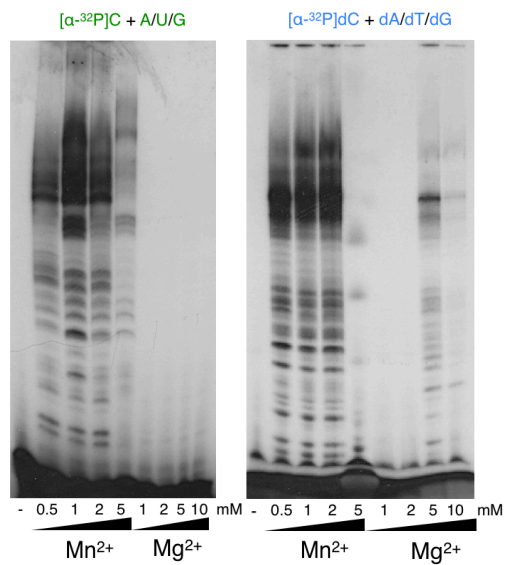
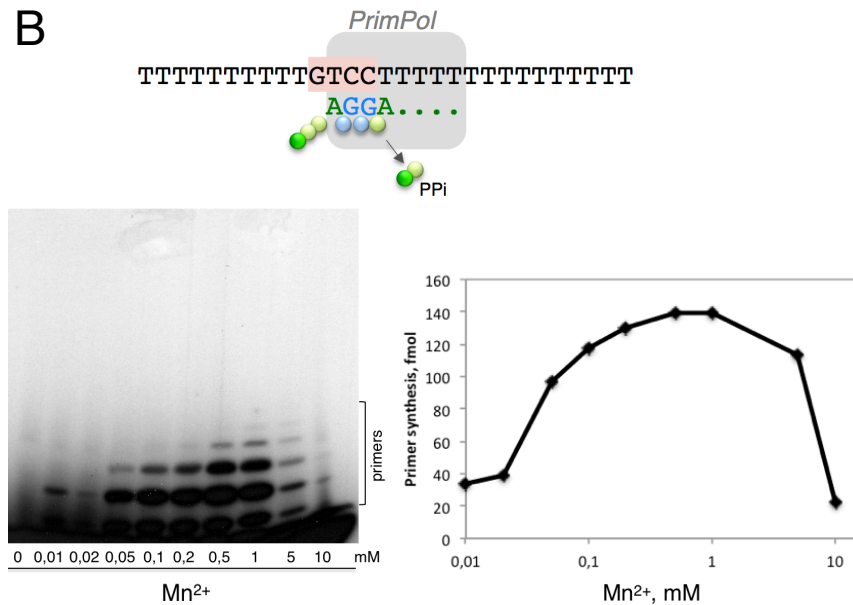
C

3' TT (T₁₀)TTTTTTTT**GTCC**TTTTTTTTTTTT(T₂₂)TTT5'



	1	2	3	4	5	6	7
[α - ³² P]dA	+	+	+	+	+	+	+
ccdc111	-	+	+	+	+	+	+
GTCC-ori	-	-	+	+	+	+	+
dC/dT/dG	-	-	-	+	+	+	+
ATP	-	-	-	-	+	-	+

Fig S2 García-Gómez et al.

A**B****C**

3'CTAGTGTCACCTCATGCTCTATGTGAAGA 5'

*5'GATCACAGTGAGTAC

dG

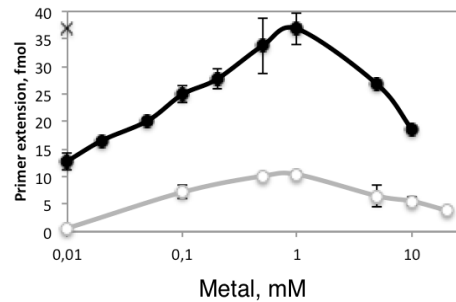
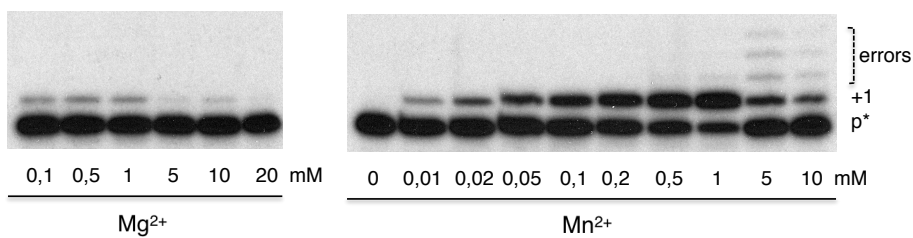


Fig S3 García-Gómez et al.

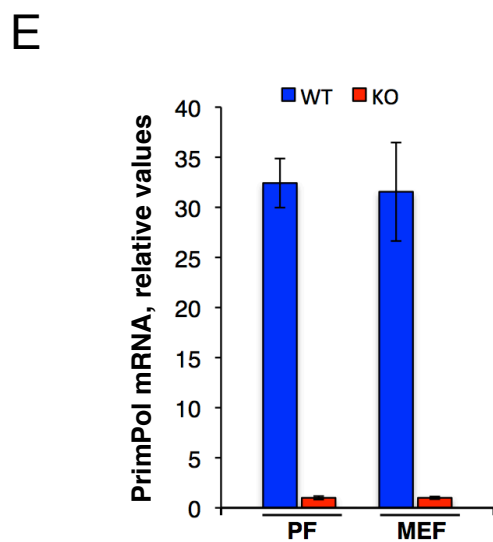
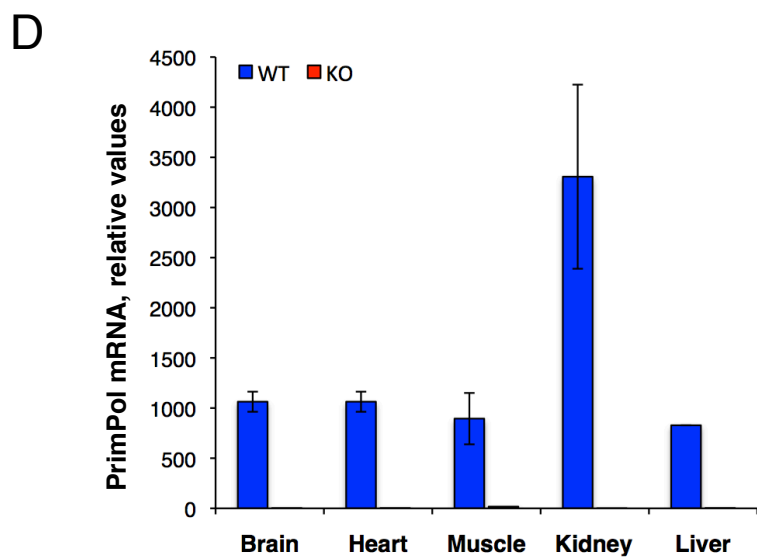
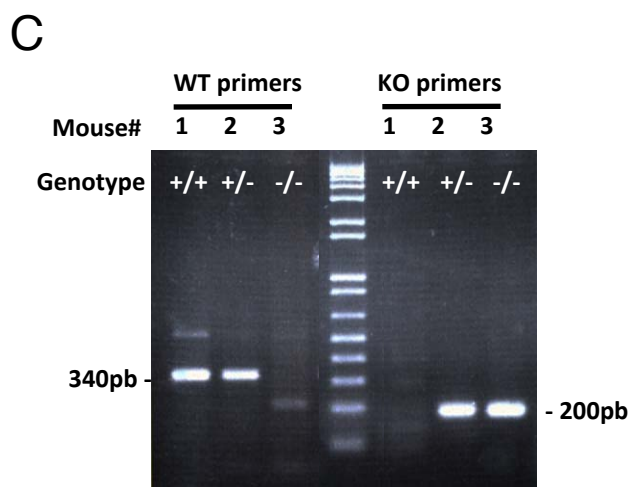
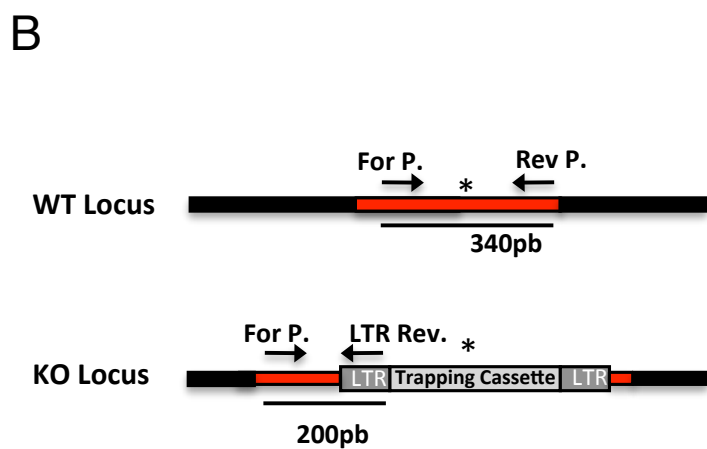
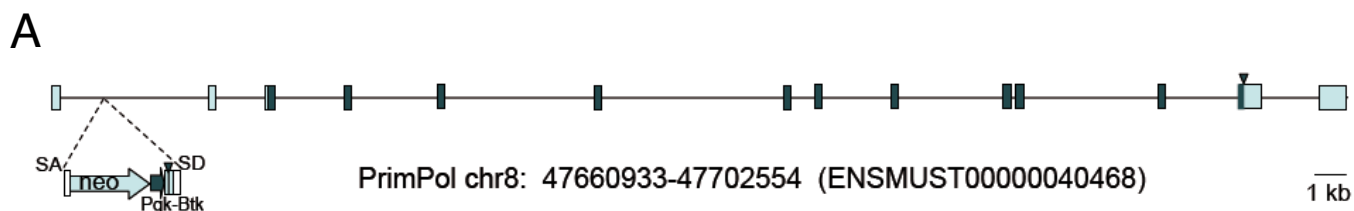
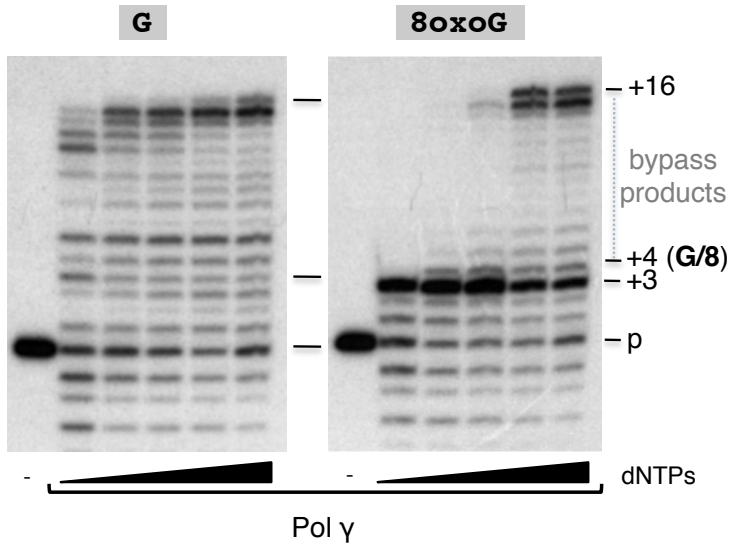


Fig S4 Garcia-Gómez et al.

A

CTAGTGTCACTCATG**X**TCTATGTGAAGA
 *GATCACAGTGAG

**B**

GTGACTGACATACTAC**X**TCTACGACTGCTC
 *CACTGACTGTATG

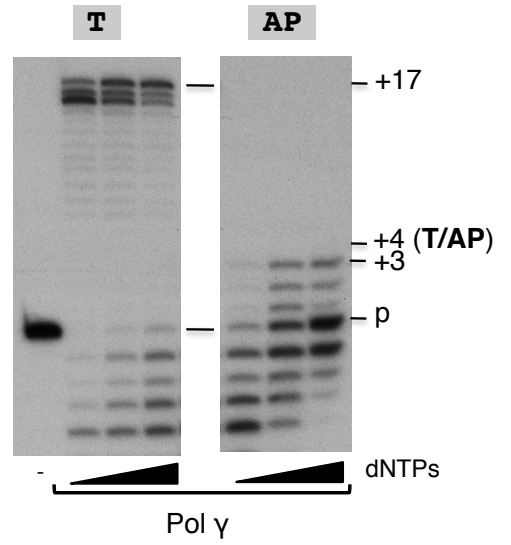


Fig S5 García-Gómez et al.

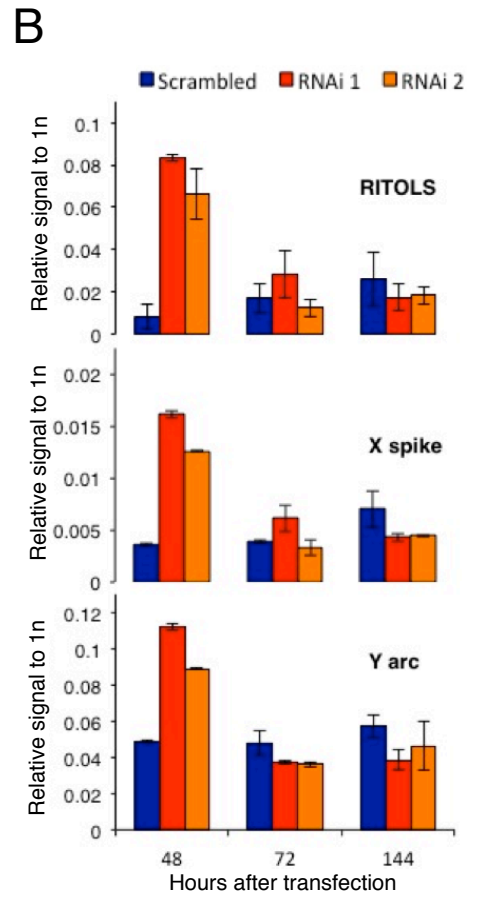
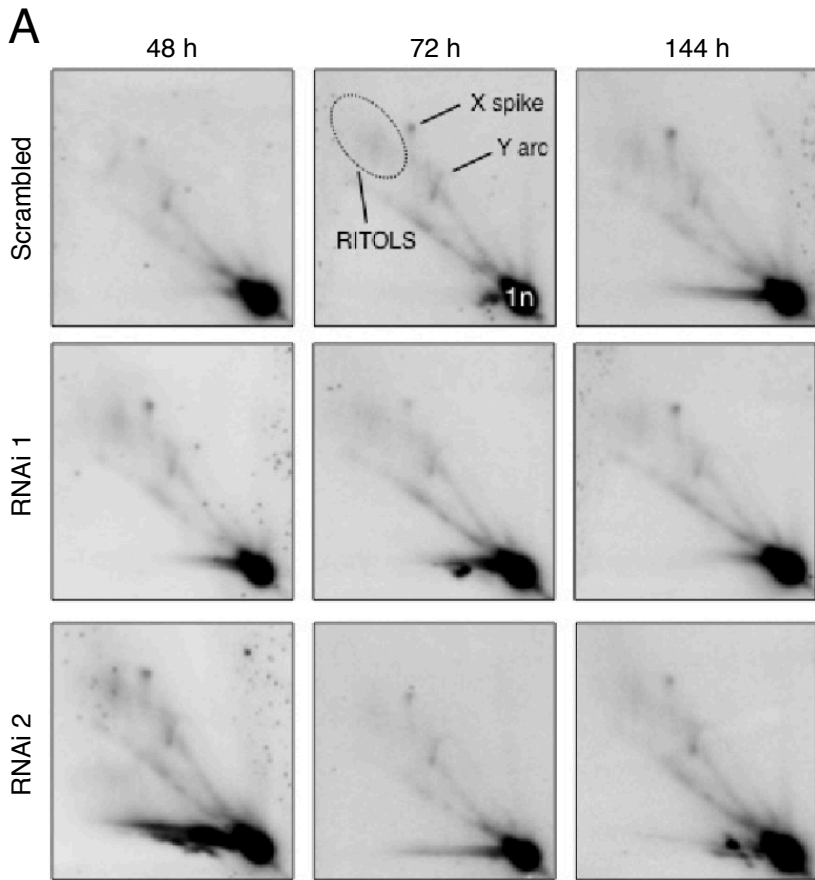


Fig S6 García-Gómez et al.

LEGENDS TO SUPPLEMENTAL FIGURES

Figure S1. The Eukaryotic ccdc111/PrimPol Family, Related to Figure 1

Multiple amino acid sequence alignment of ccdc111 orthologues. Numbers between slashes indicate the amino acid position relative to the N-terminus, and numbers in parentheses indicate the total number of amino acid residues. Invariant or highly conserved residues (red letters) or another identities conserved in most sequences (blue letters) are indicated. The alignment defines 14 conserved regions (boxed) among the ccdc111 family, including the highly conserved motifs A, B and C, characteristic of AEP-like primases, and the Zn-finger motif, characteristic of some viral primases (Iyer et al., 2005) and other AEP-related enzymes. Dots at the top of the aligned sequences indicate invariant residues acting either as metal (red), nucleotide (purple) or Zn (blue) ligands. Multiple alignments of the different members of the eukaryotic ccdc111(PrimPol) family were done using the program MULTALIN (<http://prodes.toulouse.inra.fr/multalin/>).

Figure S2. Purification of Human Ccdc111 (PrimPol), and Primase Activity in Ccdc111-Expressing Cell Extracts, Related to Figure 1

(A) SDS PAGE analysis of the different purification steps. 1: cell extract before induction; 2: cell extract after induction; 3: soluble fraction; 4: insoluble fraction 5: flow-through of the NTA-Ni agarose; 6: elution of the protein from NTA-Ni agarose; 7: elution of Heparin-Sepharose.

(B) Primase activity assay on M13 ssDNA with crude extracts, revealed by EtBr staining (upper left panel) and autoradiography (lower left panel) after agarose gel electrophoresis, or analyzed by denaturing 8M urea 20% acrylamide gel electrophoresis (right panel); 1: control with no protein, 2: non-induced cell extract, 3: ccdc111-induced cell extract; 4:

purified ccdc111 protein.

(C) Primase activity assay on an ori-containing oligonucleotide (see scheme), catalyzed by two versions of purified ccdc111 protein, expressed in *E. coli* BL21(DE3) cells: a GST-tagged construct (GST-ccdc111; left panel); a Histidine-tagged construct (His-ccdc111; right panel).

Figure S3. Metal Activators of Ccdc111/PrimPol Primase and Polymerase Activities, Related to Figures 1 & 2

(A) Manganese is the preferred metal activator for ccdc111-associated primase. The reaction mixture (in 20 μ L) was incubated as indicated in [Supplemental Experimental Procedures](#), using M13 ssDNA (10 ng/ μ L) as template and either ribonucleotides ($[\alpha$ -³²P]CTP (16 nM) + ATP/GTP/UTP (100 μ M); left panel) or deoxynucleotides ($[\alpha$ -³²P]dCTP (16 nM) + dATP/dGTP/dTTP (100 μ M); right panel), human ccdc111 protein (400 nM), and the indicated concentration (in mM) of either MnCl₂ or MgCl₂ as metal activators. After incubation for 60 min at 30 °C, primer synthesis was analyzed by 20% PAGE-8M urea and autoradiography. In the two different conditions tested, ccdc111-associated primase was largely better activated by manganese versus magnesium ions.

(B) Manganese ions concentration required for the primase activity of PrimPol. The reaction mixture (20 μ L) contained buffer R, 1 μ M oligonucleotide (5' T₁₅CCTGT₁₀ 3'), 16 nM [γ -³²P]ATP(3000 Ci/mmol), 10 μ M dGTP, 400 nM PrimPol, in the presence of the indicated concentrations of MnCl₂. After 60 min at 30 °C, reactions were stopped by addition of formamide loading buffer (10 mM EDTA, 95% v/v formamide, 0.3% w/v xylencyanol). Reactions were loaded in 8 M urea-containing 20% polyacrylamide sequencing gels. After electrophoresis, *de novo* synthesized polynucleotides (primers) were detected by autoradiography. As the primers are only labeled at their 5'-end, total

primer synthesis (in fmol) was estimated from the ratio of labeled primers *versus* total [γ - ^{32}P]ATP.

(C) Manganese and magnesium concentration required for the DNA polymerase activity of PrimPol. A 15-mer oligodeoxynucleotide primer (5' GATCACAGTGAGTAC 3') was 5"-labelled with T4 polynucleotide kinase and [γ - ^{32}P]ATP (3000 Ci/mmol), and hybridized to a 28-mer oligodeoxynucleotide template (5' AGAAGTGTATCTCGTACTCACTGT GATC 3'). The resulting hybrid has a 5'-protrusion of 13 templating nucleotides. The reaction mixture (20 μL) contained buffer R, [γ - ^{32}P]-labelled template/primer DNA (2.5 nM), 1 μM dGTP, human PrimPol (200 nM), and the indicated concentration of either Mn^{+2} (0.01, 0.02, 0.05, 0.1, 0.2, 0.5, 1, 5, 10) or Mg^{+2} (0.01, 0.1, 0.5, 1, 5, 10, 20). After 60 min of incubation at 30 $^{\circ}\text{C}$, reactions were loaded in 8 M urea-containing 20% polyacrylamide sequencing gels. After electrophoresis, the products were detected by autoradiography. Primer extension (in fmol), was estimated from the fraction of labeled primer that reached the +1 position. Data are represented as mean \pm SD (n=3).

Figure S4. Disruption of the *CCDC111* (*PRIMPOL*) gene, and generation of *PRIMPOL*^{-/-} mice, Related to Figures 4 & 6

(A) Trapping vector used to generate the PrimPol^{-/-} mice.

(B) Primers and expected size of the PCR products, used to distinguish between the WT and KO locus.

(C) Agarose gel and PCR Genotyping. Separate PCR analyses were used to distinguish the PCR products from either the wild-type (340 bp) and mutant alleles (200 bp).

(D,E) Quantitative RT-PCR indicated lack of *ccdc111* expression in five different murine tissues and cells (primary fibroblasts (PF) and MEFs) derived from the PrimPol^{-/-} mouse model. Data are represented as mean \pm SEM.

Figure S5. Deficient bypass of 8oxoG and abasic sites by human Pol γ , Related to Figure 5

(A) *In vitro* “running start” DNA polymerization by human Pol γ on a control template (left panel), or on a template containing a 8oxoG lesion (right panel). dNTPs were provided at either 0.01, 0.05, 0.1, 0.5 and 1 μ M. The position of the lesion in the template strand is marked (X) in the top schematic as well as in the autoradiogram. On the damaged template, human Pol γ efficiently extended the primer by three nucleotides (+3), but further elongation was very inefficient compared with the control template, indicating a deficient incorporation opposite the 8oxoG lesion.

(B) Same as A, but the damaged template/primer (right panel) contains an abasic site. dNTPs were provided at 1, 10, and 100 μ M. Unlike the full primer extension observed on the control template, human Pol γ extended the primer until the position preceding the abasic site (AP), and stopped synthesis.

Figure S6. Mitochondrial Replication Intermediates are transiently affected by PRIMPOL Gene Silencing, Related to Figure 6

(A) HincI-digested cellular DNA analyzed by neutral 2D-AGEs, using a radiolabelled probe spanning nucleotides 13636-1006 of the human mitochondrial genome, as previously described (Yasukawa et al., 2005). The DNA was harvested from HOS cells 48, 72 and 144 h after transfection with scrambled or PRIMPOL siRNAs (RNAi 1 and RNAi 2). Non-replicating mtDNA (1n) and different replication intermediates are marked in one of the panels as a reference: RITOLS, X spike and Y arc (for a description of the different replication intermediates see Yasukawa et al., 2005; Reyes et al., 2013).

(B) Quantitation of label in replication intermediates shown in part A, based on phosphorimaging. Values on vertical axes are based on signal from replication intermediates normalized to non-replicating (1n) signal for each time point in each sample. Data are represented as mean +/- SEM.

SUPPLEMENTAL EXPERIMENTAL PROCEDURES

Overproduction and Purification of Human *ccdc111* (PrimPol)

Plasmids construction. A full-length cDNA of the *CDCC111* human gene, located in chromosome 4 (4q35.1) was obtained from Imagenes (<http://www.imagenes-bio.org>). Overexpression of the wild-type protein cloned in the pET16a vector, without any tag, was previously attempted using *E. coli* BL21(DE3), BL21(DE3)-pLysS or BL21(DE3)-pRIL, but a degradation protein product with an estimated molecular mass of 30 kDa was obtained in all cases, revealing the instability of the protein. Therefore we tried to stabilize the protein fusing a His-tag at its N-terminus. For that, the *CCDC111* gene was amplified by PCR, and flanking *NdeI*-*Bam*HI sites were introduced to facilitate the cloning in a pET16a expression vector (Novagen), that fused a 6xHis tag to the N-terminal of the protein. The resulting plasmid was named pET16::*CCDC111* and kept in *E. coli* DH5 α . In order to verify that the protein activities were intrinsic to *ccdc111*, a mutant in the predicted primase active site was also designed and constructed using the Quick Change Site Directed Mutagenesis kit from Stratagene, using plasmid pET16::*CCDC111* to obtain plasmid pET16::AXA (encoding a double-mutant *ccdc111* protein, in which both Asp¹¹⁴ and Glu¹¹⁶ are changed to alanines). Over-expression of the His-tagged wild-type and mutant protein in *E. coli* BL21(DE3)-pRIL gave rise to a 67 kDa protein product that corresponded to the predicted protein mass. A N-terminal fusion with GST was also constructed, and the

overproduced GST-ccdc111 was stable and showed the same enzymatic characteristics as His-ccdc111. The protein used throughout this study was the His-tagged ccdc111.

Purification of human ccdc111. Protein expression and purification was performed identically for the wild-type and the mutated AXA protein. *E. coli* BL21(DE3)-pRIL cells were transformed with the expression plasmid pET16::CCDC111 or pET16::AXA. An overnight culture was incubated at 37 °C and used to inoculate 2L of LB + Amp and Cm. Cells were grown at 30 °C up to OD₆₀₀ 0.8, and then induced with 1 mM IPTG for 2 h and 30 min. Cells were harvested at 12000 xg for 5 min at 4°C, and the resulting bacterial pellet (3 g/L) was frozen at -20°C. 6 g of cells were resuspended in 100 mL lysis buffer [buffer A (50 mM Tris-HCl pH 8, 1 M NaCl, 10% glycerol, 1 mM PMSF, 2 mM β-mercaptoetanol, 10 mM imidazol and 400 mM AcNH₄) and lysated by 10 min sonication pulses. The lysate was centrifuged at 27000 xg for 30 min at 4°C to remove cell debris. 60% of the protein remained in the pellet, and was used to obtain polyclonal antibodies against ccdc111, whereas the remaining fraction (soluble) was further purified. Supernatant was bound in batch with 2 mL Ni-NTA Agarose (Qiagen) during 2 h at 4°C. Resin was washed in batch with the lysis buffer and packed into a column, then washed with 40 column volume of buffer A and other 40 vol of buffer A with 20 mM imidazol. Before elution, the resin was equilibrated with buffer B (50 mM Tris-HCl pH 8, 10% glycerol, 1 mM PMSF, 2 mM β-mercaptoetanol) and 50 mM NaCl, and then protein was eluted with buffer B supplemented with 50 mM NaCl and 200 mM imidazol. Fractions containing the ccdc111 protein were loaded in a Heparin Sepharose column (GE Healthcare), washed with 10 vol of buffer B with 50 mM NaCl, then with 10 vol of buffer B with 100 mM NaCl, and finally eluted with buffer B and 1 M NaCl. Fractions containing the purified His-ccdc111 protein were stored at -20°C in buffer C (50 mM Tris-HCl pH 8, 50% glycerol, 500 mM NaCl and 1mM DTT). The His-ccdc111 protein purified under these

conditions yielded 1 mg/L of cell culture, and was stable for 6-10 months. A representative summary of the purification procedure is shown in [Figure S2A](#).

Obtention of polyclonal antibodies against human PrimPol. Protein antigen corresponding to human *ccdc111* (PrimPol) protein antigen was obtained from *E. coli* BL21(DE3) pRIL cells. After IPTG induction, the insoluble fraction of the lysate (containing a high proportion of the expressed PrimPol) was treated with 6 M urea, and the denatured protein was bound to Ni-NTA (Qiagen). The column was washed with 20 mM imidazol and then, PrimPol was eluted with 200 mM imidazol, and quantified. Two New Zealand rabbits were inoculated 3 times with 0.5 mg of the purified *ccdc111* human protein and Freund's adjuvant. Polyclonal antiserum was obtained, and the PrimPol-specific IgG fraction was affinity-purified following standard procedures.

A second antibody against human PrimPol was obtained by inoculation of New Zealand rabbits with a peptide corresponding to the last 14 C-terminal amino acids (DEIPDELIIEVLQE) of human PrimPol. These antibodies were shown to be very effective for a clean detection of human PrimPol by western blotting of crude cell fractions.

Early Detection of Human Ccdc111 (PrimPol) Specific Activity

Ccdc111-dependent primase activity overproduced in E. coli cells. As a first indication that *ccdc111* is an active primase, we assayed the total primase activity present in control cell extracts versus *ccdc111*-overproducing extracts (0.8 $\mu\text{g}/\mu\text{L}$), using M13 ssDNA as template (10 $\text{ng}/\mu\text{L}$), 1 mM MnCl_2 , 10 μM of ATP, GTP and UTP, and 16 nM of [α - ^{32}P]CTP to label the primase products in a 20 μL reaction. After incubation for 60 min at 30 °C, a half of the reaction was analyzed by agarose gel electrophoresis ([Fig. S2B](#), left panels), and the other half in denaturing conditions by 20% acrylamide/8M urea gel electrophoresis ([Fig. S2B](#), right panel). Only when using *ccdc111* overproducing extracts ([Fig. S2B](#), lane

3), but not with control extracts (Fig. S2B, lane 2), a radioactive band was observed under native conditions, associated to the M13 ssDNA band (stained by EtBr). A similar reaction was obtained with purified *ccdc111* protein (0.4 μ M; Fig. S2B, lane 4). This band represents *de novo* synthesis of RNA (primase activity) annealed to the M13 template. The undetectable primase activity in the control cell extracts indicates that the endogenous *E. coli* DnaG primase is not in a sufficient amount in the reaction to give any background signal. The size of the newly synthesized oligonucleotides that emerged from the primase reaction was analyzed under denaturing conditions (Figure S2B, right panel).

DNA primase activity is ccdc111-specific, irrespective of the tagged-version and purification source. Ccdc111-associated DNA primase activity was tested on a 60-mer oligonucleotide rich in thymidine residues, but containing a putative “ori” sequence (GTCC) at a central position (see scheme at Fig. S2C). To demonstrate that GTCC-ori recognition (and the primase itself) is intrinsic to *ccdc111*, the experiments were carried out with 2 different versions of *ccdc111*, overproduced in *E. coli* BL21(DE3) cells: a GST-tagged construct (GST-*ccdc111*; left panel); a Histidine-tagged construct (His-*ccdc111*; right panel). The complete reaction mixture (in 20 μ L) contained 1 μ M of the GTCC-containing oligo (ori) as template, 1 mM MnCl_2 , [α - ^{32}P]dATP (16 nM), dGTP/dCTP/dTTP (10 μ M), ATP (1 mM), and human *ccdc111* protein (400 nM) from the two different sources indicated above. Some of the components were omitted as indicated. After incubation for 60 min at 30 °C, primer synthesis was analyzed by 20% PAGE-8M urea and autoradiography. Some background labeling was observed in the absence of the template (ori) when providing only [α - ^{32}P]dATP and *ccdc11* (lane 2). New labeled bands were observed when additionally providing the ori oligonucleotide (lanes 3), suggesting that perhaps these are primase-made products starting somewhere at the T-rich region (as dATP is the only nucleotide provided). However, *bona fide* primase initiating products

(ranging from 2 nucleotides; indicated with a white frame) were observed by additionally providing the three remaining dNTPs (lanes 4 and 6). Finally, addition of ATP 1mM (lanes 5 and 7) boosted both initiation and elongation giving rise to longer primer molecules. These products were very similar, irrespective of the tagged-version and purification protocol of *ccdc111*, suggesting that the primase activity is *ccdc11*-specific.

Primase assays on specific oligonucleotide templates

As a more specific template to assay primase activity, we used either the 60-mer GTCC oligonucleotide: 5' T₃₆CCTGT₂₀ 3', or the 29-mer GTCC: 5' T₁₅CCTGT₁₀ 3', both containing a putative herpes virus priming initiation site (Cavanaugh and Kuchta, 2009). The reaction mixture (20 μ L) was carried out in buffer R (when indicated, various concentrations of MnCl₂ were used to define the range of metal activation), GTCC oligonucleotide (1 μ M), labelled nucleotide (16 nM; 3000 Ci/mmol; either [α -³²P]ATP, [α -³²P]dATP or [γ -³²P]ATP), 10 μ M dGTP or GTP, in the presence of human PrimPol (400 nM) WT or AxA mutant. When indicated, PrimPol was either used at different concentrations, or substituted by other DNA polymerases or conventional primases. After 60 min at 30 °C, reactions were loaded in 8 M urea-containing 20% polyacrylamide sequencing gels. After electrophoresis, *de novo* synthesized polynucleotides (primers) were detected by autoradiography.

Manganese is the preferred metal activator for both the primase and DNA polymerase activities of PrimPol

The effect of the metal ion in the efficiency *versus* fidelity of nucleotide incorporation is a relevant and physiological issue. In general, DNA replicases use Mg⁺² to have the maximal insertion fidelity. Conversely, other polymerases are tailored to maximize efficiency (not

fidelity) of catalytically difficult reactions, as the primase initiation reaction (by PrimPol) or NHEJ of incompatible ends (by Pol μ), by using Mn⁺² ions that boost nucleotide binding at their active sites. An extreme example is TdT, a close Pol μ homologue, able to use Mg⁺², Mn⁺² or even Co⁺² to catalyze template-independent nucleotidyltransferase reactions on different primer configurations. Thus, it appears that PrimPol, like some other DNA polymerases involved in translesion synthesis and DNA repair, as Pol mu (Domínguez et al., 2000), Pol lambda (Blanca et al., 2003), Dpo4 (Vaisman et al., 2005), and Pol iota (Frank et al., 2007), has a preference for activating Mn⁺² ions instead of the more conventional Mg⁺² ions.

When assayed *in vitro* on M13 ssDNA as template, PrimPol primase activity has an optimum of 1 mM Mn⁺², much higher than the physiological concentration of this trace metal (Figure S3A). Interestingly, although 1 mM is the optimal Mn⁺² concentration, PrimPol can use much lower (20-fold) concentration of Mn⁺² ions (50 μ M) to efficiently catalyze its primase activity (Figure S3B). It has been discussed for a long time the physiological role of the Mn⁺² ions particularly during oxidative stress (Aguirre and Culotta, 2012). Interestingly, the levels of intracellular manganese can increase up to 1-3 mM in some bacteria, as a response to genotoxic damage (Tseng et al., 2001; Slade and Radman, 2011). Moreover, mitochondria under oxidative stress uptakes high concentrations of Mn⁺² ions (Gunter et al., 2009).

As it happened for the primase activity, when the metal requirements for the DNA polymerase activity of PrimPol are analyzed using a primer extension assay, the optimal Mn⁺² concentration is 1 mM; however, PrimPol can use much lower (100-fold) concentration of Mn⁺² ions (10 μ M) to efficiently catalyze its DNA polymerase activity (Figure S3C). Interestingly, Mg⁺² ions were much less efficient at any concentration tested. In fact, the DNA polymerase activity at a physiological concentration of 10 mM Mg⁺² was

less efficient than that obtained with 0.1 mM Mg⁺². Moreover, the lowest concentration of Mn⁺² tested (10 μM), in or even below the physiological range, was more efficient than a physiological concentration of Mg⁺² ions (10 mM). A very similar behaviour has been described for human Polλ (Blanca et al., 2003). These data reinforce the biological significance of the preference of human PrimPol for Mn⁺² ions.

Antibodies used after Iodixanol gradient fractionation of purified mitochondria

Mouse anti-RNASEH1 (1:1000 Abcam); goat anti-POLG1 (1:500 Santa Cruz); rabbit anti-SSP1 (1:500 Abcam); rabbit anti-HSP60 (1:3000 Abcam); rabbit anti-TOM20 (1:2000 Abcam); rabbit anti-POLRMT (1:1000 Abcam); rabbit anti-VDAC1 (1:20000 Abcam); rabbit anti-ETFB (1:15000 Proteintech); rabbit anti-TIM23 (1:1000 Sigma). Mouse anti-TWINKLE (1:200) and rabbit anti-TFAM (1:40000) were kind gifts of A. Soumalainen and R.J. Wiesner, respectively. Rabbit anti-PrimPol (1:1000) and rabbit anti-POLG2 were raised against recombinant proteins produced in-house. Secondary antibodies were anti-mouse, anti-goat or anti-rabbit HRP 1:1000 (Promega).

Stealth RNA sequences used for siRNA-mediated depletion of PrimPol.

Double-stranded RNAs were:

(RNAi 1): 5'-GAGGAAACCGUUGUCCUCAGUGUAU-3' and 5'-
AUACACUGAGGACAACGUUCCUC-3'

(RNAi 2): 5'-CACCCUCCAUCUGGAGACUAUUUCA-3' and 5'-
UGAAAUAGUCUCCAGAUGGAGGGUG-3'

(RNAi 3): 5'-UUCCAAAGCAAUACAUGAACGUCU-3' and 5'-
AGACGUUCAUGUAUUUGCUUUGGAA-3'

Disruption of the *CCDC111* (*PRIMPOL*) gene and generation of *PRIMPOL*^{-/-} mice

PRIMPOL-deficient mouse generation and genotyping. To generate the *PRIMPOL*-KO mouse, the Omnibank (Lexicon, Woodlands, Texas) database was searched with the mouse *ccdc111* reference cDNA sequence (NM_001001184) and 4 clones were identified. The ES clone OST296220 had an insertion of the trapping retroviral vector VICTR48 (Zambrowicz et al., 1998) in the first intron of the *CCDC111* gene (reference sequence ENSMUST00000040468). The trapping vector (see scheme in Figure S4A) contains a promoterless *neo* expression cassette preceded by splice-acceptor sequence and followed by a *Pgk*-promoter driven *Btk* exon-splice donor cassette with three-frame stop codons. Thus, the insertion is predicted to result in the efficient trapping of the *CCDC111* promoter to generate neo-fusion transcripts missing all coding exons (3-13). Downstream to the insertion, the *Pgk* promoter would drive the expression of the *Btk* exon fused to exons 2-14, but containing early stop codons in all reading frames, which would trigger nonsense mediated mRNA decay. ES cells were then injected into C57Bl6 blastocysts at TIGEM, and chimeric males were used to generate progenies that included ES-derived mice, heterozygous for the trapping insertion at the *CCDC111* (*PRIMPOL*) gene. These *PRIMPOL*^{+/-} mice were used to generate an intercross colony, with mixed 129 and C57Bl6 background. Crosses were followed by genotyping tail-tip DNA, using polymerase chain reaction (PCR) with primers PrimPol-F (5'-cctacatctgcaagaagacttagc) and PrimPol-R (5'-acactgggtccctttacagatgg) and LTR-R (5'-ataaacctcttgcagttgcatc) (Figure S4B), and temperature profile of 20" at 94°C, 20" at 55°C, 20" at 72°C), for 35 cycles. Agarose electrophoresis of PCR products (Figure S4C) yields a 340 bp product for the wild type allele (primers F&R) and a 200 bp product for the trapped allele (primers F<R-R). The

resulting *PRIMPOL*^{-/-} mice are viable and fertile, and are described and used in this study for the first time.

PRIMPOL mRNA relative expression levels. A PrimPol-specific antibody against the mouse protein is not currently available in our laboratory. Thus, we used quantitative PCR (qPCR) to evaluate *PRIMPOL* mRNA expression levels in *PRIMPOL*-null versus wild-type mice. qPCR was performed from total RNA extracts obtained by standard procedures either from mouse tissues or from mouse primary (PF) or embryonic (MEF) fibroblasts. First, reverse transcription (RT) of total RNA was performed followed by qPCR to quantify relative levels using an ABI PRISM 7900 HT SDS systems (Applied Biosystems). Power Syber Green PCR Master mix (ABI) was used for all the samples. An initial denaturation of 30'' at 95°C followed by 40 two-step cycles (5'' at 95°C, 5'' at 60°C) was performed for all the genes evaluated. A final melting ramp curve from 60°C to 95°C (0.5 °C/seg) was also included in order to verify the amplification products. The primers used for *PRIMPOL* were *PRIMPOL*-F (5'-ctggtgagcaatgtcagattct) and *PRIMPOL*-R (5'-gccgaatccctcctttaatgt), with an intron-spanning design in order to avoid genomic DNA amplification. Two housekeeping genes (HPRT and 18S) were used for every assay in order to correct for loading errors. Data analysis was performed using the GenEx software, as described (Livak et al., 2001).

We assessed mRNA levels in different tissues from both *PRIMPOL*^{+/+} (WT) and *PRIMPOL*^{-/-} (KO) mice. PrimPol was highly expressed (5-fold) in kidney from WT mice, compared to other tissues such as liver, heart brain or muscle (Figure S4D). PrimPol mRNA levels in KO mice were barely undetectable in any of these tissues. Similar results were observed when assaying PrimPol WT *versus* KO cells derived from these mice, such as adult primary (PF) or embryonic (MEF) fibroblasts (Figure S4E). These results demonstrate the lack of expression of the *CCDC111* gene in *PRIMPOL*^{-/-} mice.

Mouse mtDNA strand-specific riboprobes used in fragmentation analysis of mtDNA.

Riboprobes were generated from amplified mouse mtDNA containing a T7 promoter and an *in vitro* transcription kit (Ambion). H-strand and L-strand specific probes were nt 15,811-16,034 and nt 15,750-16,030, respectively.

SUPPLEMENTAL REFERENCES

- Aguirre, J.D. and Culotta, V.C. (2012) Battles with iron: manganese in oxidative stress protection. *J. Biol. Chem.* *287*, 13541-13548.
- Blanca, G., Shevelev, I., Ramadan, K., Villani, G., Spadari, S., Hübscher, U. and Maga, G. (2003). Human DNA polymerase lambda diverged in evolution from DNA polymerase beta toward specific Mn(++) dependence: a kinetic and thermodynamic study. *Biochemistry* *42*, 7467–7476.
- Cavanaugh, N.A. and Kuchta, R.D. (2009). Initiation of new DNA strands by the herpes simplex virus-1 primase-helicase complex and either herpes DNA polymerase or human DNA polymerase alpha. *J. Biol. Chem.* *284*, 1523–1532.
- Domínguez, O., Ruiz, J.F., García-Díaz, M., Laín, M., González, M., Martínez-A, C., Bernad, A. and Blanco, L. (2000) DNA polymerase mu (Pol μ), homologous to TdT, could act as a DNA mutator in eukaryotic cells. *The EMBO J.* *19*, 1731-1742.
- Frank, E.G. and Woodgate, R. (2007) Increased catalytic activity and altered fidelity of human DNA polymerase iota in the presence of manganese. *J. Biol. Chem.* *282*, 24689-24696.
- Gunter, T.E. Gavin, C.E. and Gunter, K.K. (2009) The Case for Manganese Interaction with Mitochondria. *Neurotoxicology* *30*, 727-729.

- Iyer, L.M., Koonin, E.V., Leipe, D.D. and Aravind, L. (2005). Origin and evolution of the archaeo-eukaryotic primase superfamily and related palm-domain proteins: structural insights and new members. *Nucleic Acids Res.* *33*, 3875-3896.
- Livak, K.J. and Schmittgen, T.D. (2001) Analysis of relative gene expression data using real-time quantitative PCR and the 2(-Delta Delta C(T)) Method. *Methods* *25*, 402-440.
- Reyes, A., Kazak, L., Wood, S.R., Yasukawa, T., Jacobs, H.T. and Holt, I.J. (2013) Mitochondrial DNA replication proceeds via a “bootlace” mechanism involved the incorporation of processed transcripts. *Nucleic Acids Res.* [Epub ahead of print] PMID: 23595151.
- Slade, D. and Radman, M. (2011). Oxidative stress resistance in *Deinococcus radiodurans*. *Microbiol. Mol. Biol. Rev.* *75*,133-191.
- Tseng, H.J., Srikhanta, Y., McEwan, A.G. and Jennings, M.P. (2001). Accumulation of manganese in *Neisseria gonorrhoeae* correlates with resistance to oxidative killing by superoxide anion and is independent of superoxide dismutase activity. *Mol. Microbiol.* *40*, 1175–1186.
- Vaisman, A., Ling,H., Woodgate, R. and Yang, W. (2005) Fidelity of Dpo4: effect of metal ions, nucleotide selection and pyrophosphorolysis. *The EMBO Journal* (2005) *24*, 2957–2967.
- Yasukawa, T., Yang, M.Y., Jacobs, H.T. and Holt, I.J. (2005). A bidirectional origin of replication maps to the major noncoding region of human mitochondrial DNA. *Mol. Cell.* *18*, 651-662.
- Zambrowicz, B.P., Friedrich, G.A., Buxton, E.C., Lilleberg, S.L., Person, C. and Sands, A.T. (1998) Disruption and sequence identification of 2,000 genes in mouse embryonic stem cells. *Nature* *392*, 608-611.